

# The effect of water on the activity and selectivity for $\gamma$ -alumina supported cobalt Fischer–Tropsch catalysts with different pore sizes

Øyvind Borg<sup>a</sup>, Sølvi Storsæter<sup>a,b</sup>, Sigrid Eri<sup>b</sup>, Hanne Wigum<sup>b</sup>, Erling Rytter<sup>b</sup>, and Anders Holmen<sup>a,\*</sup>

<sup>a</sup>Department of Chemical Engineering, Norwegian University of Science and Technology (NTNU), NO-7491, Trondheim, Norway

<sup>b</sup>Statoil R&D, Research Centre, Posttuttak, NO-7005, Trondheim, Norway

Received 16 November 2005; accepted 24 November 2005

The effect of water on the activity and selectivity for a series of  $\gamma$ -Al<sub>2</sub>O<sub>3</sub> supported cobalt Fischer–Tropsch catalysts has been studied in an isothermal fixed-bed reactor at  $T=483$  K,  $P=20$  bar, and  $H_2/CO=2.1$ . The catalysts were produced applying incipient wetness impregnation and consisted of 20 wt.% cobalt and 0.5 wt.% rhenium deposited on  $\gamma$ -Al<sub>2</sub>O<sub>3</sub> supports with different pore characteristics. For the narrow-pore catalysts, addition of water corresponding to an inlet partial pressure ratio of  $P_{H_2O}/P_{H_2}=0.4$  reduced the reaction rates. In contrast, for a catalyst with larger pores the same water pressure increased the reaction rates. For all catalysts, water amounts equal to  $P_{H_2O}/P_{H_2}=0.7$  at the reactor inlet suppressed the reaction rates and led to permanent deactivation. The addition of water increased the C<sub>5+</sub> selectivity and decreased the CH<sub>4</sub> selectivity for all catalysts. The pore characteristics seem to determine the effect of water on the rates.

**KEY WORDS:** Fischer–Tropsch synthesis; cobalt; rhenium; alumina; water; pore size.

## 1. Introduction

Supported cobalt is considered to be the most favourable catalytic material for synthesis of long-chain hydrocarbons from natural gas-based synthesis gas due to its high activity, high selectivity for linear paraffins, low water–gas shift activity, and relatively low price compared to noble metals.

Since oxygen mainly is rejected as water during Fischer–Tropsch synthesis on cobalt catalysts, water will always be present during reaction. The presence of water may influence the reaction rate, the product distribution, and the deactivation rate. For this reason, several studies of the impact of water have been carried out. However, depending on the support different results regarding the effect of water on the catalyst activity have been reported. It has been observed that the activity may decrease [1–21] or even increase as a result of water either added to the feed or produced by the reaction [8,9,22–31]. For some catalytic systems no effect of water on the activity was observed [32].

The influence of water on  $\gamma$ -Al<sub>2</sub>O<sub>3</sub> supported catalysts has been subject of several studies. Schanke *et al.* [3,4] found that the presence of large amounts of water suppressed the activity of unpromoted as well as promoted cobalt supported on  $\gamma$ -Al<sub>2</sub>O<sub>3</sub>. From X-ray photoelectron spectra, Schanke *et al.* [3,4] concluded that reoxidation of surface cobalt atoms or highly dispersed cobalt phases, and not bulk cobalt oxidation, was

responsible for the loss in activity. Hilmen *et al.* [5–7] also observed a loss in activity when water was introduced to unpromoted and promoted cobalt deposited on  $\gamma$ -Al<sub>2</sub>O<sub>3</sub>. It was also observed by Schanke *et al.* [3], Hilmen *et al.* [5,6], and Storsæter *et al.* [8] that the rhenium-promoted catalysts lost activity more rapidly than their unpromoted counterparts.

Deactivation of alumina supported cobalt catalysts during Fischer–Tropsch synthesis has been studied by steady-state isotopic transient kinetic analysis. According to Rothaemel *et al.* [10], deactivation is caused by the loss of active sites, whereas the site activity of the remaining sites is unchanged by the water treatment. This indicates that oxidation of exposed cobalt atoms is the main course for the deactivation process.

Deactivation of Pt-, Ru-, and unpromoted Co/ $\gamma$ -Al<sub>2</sub>O<sub>3</sub>, was analysed by X-ray Absorption Spectroscopic (XAS) techniques by Jacobs *et al.* [11]. X-ray Absorption Near Edge Structure (XANES) analysis gave evidence of oxidation of a fraction of the cobalt clusters to cobalt aluminate-like species by water produced during the reaction. Only the small clusters interacting with the support and clusters deviating from bulk-like behaviour were oxidised. However, Extended X-ray Absorption Fine Structure (EXAFS) results also strongly suggested that a large part of the deactivation was caused by sintering. Sintering has also been proposed as an explanation for the deactivation of a CoRe/ $\gamma$ -Al<sub>2</sub>O<sub>3</sub> catalyst [12]. Jacobs *et al.* [13] studied the effect of water on Co/ $\gamma$ -Al<sub>2</sub>O<sub>3</sub> catalysts containing 15 and 25 wt.% Co. These catalysts exhibited important differences in the degree of

\*To whom correspondence should be addressed.

E-mail: anders.holmen@chemeng.ntnu.no

cobalt interactions with the support surface. For the 15 wt.% Co/ $\gamma$ -Al<sub>2</sub>O<sub>3</sub> catalyst, which consisted of cobalt clusters between 5 and 6 nm, the oxidation likely included reaction with the support resulting in cobalt aluminate-like species. For the 25 wt.% Co/ $\gamma$ -Al<sub>2</sub>O<sub>3</sub> catalysts, the oxidation by water for the larger clusters (>10 nm) may be caused by surface oxidation to CoO. The catalysts with smaller cluster sizes were found to be more sensitive to permanent deactivation by water.

The amount of water during the Fischer–Tropsch synthesis also seems to play a significant role. By using Mössbauer emission spectroscopy, van Berge *et al.* [14] found strong indications that oxidation of reduced cobalt catalysts occurred at Fischer–Tropsch synthesis conditions. According to van Berge *et al.* [14], the degree of oxidation of the  $\gamma$ -Al<sub>2</sub>O<sub>3</sub> supported catalyst depended on the  $P_{\text{H}_2\text{O}}/P_{\text{H}_2}$  ratio. Formation of both reducible and less reducible cobalt oxide was observed, and the relative ratio between these species was affected by the severity of the oxidation conditions.

Li *et al.* [15] investigated the effect of water for a platinum-promoted Co/ $\gamma$ -Al<sub>2</sub>O<sub>3</sub> catalyst during Fischer–Tropsch synthesis in a continuously stirred tank reactor. The catalyst lost activity in the presence of water, and it was found that small quantities of water (3–25 vol.%) led to mild reversible deactivation, whereas large amounts of water (>28 vol.%) deactivated the catalyst permanently. Jacobs *et al.* [16] used XAS to define the role of water for the activity in the two partial pressure regimes. In the low partial pressure regime (< 25 vol.%), XANES scans showed that the structure of cobalt remained intact. In contrast, at higher water concentrations (>25 vol.%), XANES scans indicated formation of species chemically resembling cobalt aluminate.

The effect of water on the Fischer–Tropsch synthesis product distribution is generally accepted. For  $\gamma$ -Al<sub>2</sub>O<sub>3</sub>, as well as for other supports, the selectivity to long-chain hydrocarbons (C<sub>5+</sub>) increases and the CH<sub>4</sub> selectivity decreases as the water amount in the reactor increases [7–9,22–27,30–32]. Different explanations have been proposed to explain this effect, including the reduction of secondary hydrogenation of primary olefins by water [7,31,33]. This facilitates olefin readsorption and, therefore, in turn, further chain initiation. Recently, Bertole *et al.* [34] have suggested that the rate of propagation to termination during chain-growth in Fischer–Tropsch synthesis is strongly correlated with the steady-state amount of active surface carbon for all carbon numbers and that the dominant form of carbon is monomeric. They have concluded that most of the effects of changes in CO and water partial pressure on the chain-growth probability appear to arise via an indirect effect on the carbon inventory.

Recent studies [8,9] have also shown that the effect of water seems to depend on the structure of the support (Al<sub>2</sub>O<sub>3</sub>, SiO<sub>2</sub>, TiO<sub>2</sub>) or the size/appearance of the cobalt crystallites. The purpose of the present investigation was

therefore to study the effect of water on the activity and selectivity for a number of cobalt catalysts using  $\gamma$ -Al<sub>2</sub>O<sub>3</sub> supports with different pore characteristics. The effect of water was studied by increasing the CO conversion, more precisely from 20–35 to approximately 50 percent. In this way, the partial pressure of water in the reactor was markedly increased. In addition, the influence of water was investigated by cofeeding external water with synthesis gas. All the catalysts were subjected to exactly the same reactor setup and gaseous environment during synthesis.

## 2. Experimental

### 2.1. Catalyst preparation

A series of five supported catalysts (C-1 to C-5) containing 20 wt.% Co and 0.5 wt.% Re was prepared by one-step incipient wetness co-impregnation of different  $\gamma$ -Al<sub>2</sub>O<sub>3</sub> supports (S-1 to S-5) with aqueous solutions of cobalt nitrate hexahydrate (Acros Organics, 99%) and perrhenic acid (Alfa Aesar, 75–80%). The supports were all Puralox  $\gamma$ -Al<sub>2</sub>O<sub>3</sub> materials from Sasol.

The supports were calcined at 773 K for 10 h prior to impregnation. A temperature gradient of 1 K/min was used to ramp the temperature from room temperature to the final calcination temperature.

After impregnation, the catalysts were dried for 3 h in an oven kept at 383 K. Calcination at 573 K for 16 h in flowing air completed the preparation process. The temperature was increased by 2 K/min from room temperature to 573 K. Further pretreatment was done *in situ*.

### 2.2. Support and catalyst characterisation

#### 2.2.1. X-ray diffraction

X-ray diffraction patterns were recorded at room temperature by a Siemens D5005 X-ray diffractometer using CuK $\alpha$  radiation ( $\lambda$ =1.54 Å). The scans were recorded in the  $2\theta$  range between 10 and 90° using a step size of 0.04°. The samples (53–90  $\mu$ m) were crushed prior to measurement.

The Co<sub>3</sub>O<sub>4</sub> particle size was converted to the corresponding cobalt metal particle size according to the relative molar volumes of metallic cobalt and Co<sub>3</sub>O<sub>4</sub>. The resulting conversion factor for the diameter  $d(\text{Co}_3\text{O}_4)$  of a given Co<sub>3</sub>O<sub>4</sub> particle being reduced to metallic cobalt is [36],

$$d(\text{Co}^0) = 0.75 \cdot d(\text{Co}_3\text{O}_4) \quad (1)$$

It is known, however, that cobalt oxide particles may crack during reduction in H<sub>2</sub> [37], and in such a case relation (1) is not valid.

#### 2.2.2. Nitrogen adsorption/desorption

Nitrogen adsorption–desorption isotherms were measured with a Micromeritics TriStar 3000 instrument,

and the data were collected at liquid nitrogen temperature, 77 K. The samples (0.1–0.3 g, 53–90  $\mu\text{m}$ ) were outgassed at 573 K overnight prior to measurement.

The surface area was calculated from the Brunauer–Emmett–Teller (BET) equation [38], while the total pore volume and the average pore size were calculated from the nitrogen desorption branch applying the Barrett–Joyner–Halenda (BJH) method [39].

### 2.2.3. Hydrogen chemisorption

Hydrogen adsorption isotherms were recorded on a Micromeritics ASAP 2010 unit at 312 K. The samples (0.3–0.5 g, 53–90  $\mu\text{m}$ ) were evacuated at 312 K for 1 h, and then reduced in flowing hydrogen at 623 K for 16 h. The temperature was increased at 1 K/min from 312 to 623 K. After reduction, the samples were evacuated for 1 h at 603 K and for 30 min at 373 K, before subsequently cooling to 312 K. An adsorption isotherm was recorded at this temperature, in the pressure interval ranging from 20 to 510 mmHg. The amount of chemisorbed hydrogen was determined by extrapolating the straight-line portion of the difference isotherm to zero pressure. Furthermore, in order to calculate the dispersion, it was assumed that two cobalt sites are covered by one hydrogen molecule [40], and that rhenium did not contribute to the amount of hydrogen adsorbed [36].

The cobalt metal particle size ( $d(\text{Co}^0)$  nm) was calculated from the cobalt metal dispersion ( $D$ , %) by assuming spherical, uniform cobalt metal particles with site density of 14.6 atoms/nm<sup>2</sup>. These assumptions give the following formula [40],

$$d(\text{Co}^0) = \frac{96}{D} \quad (2)$$

### 2.3. Activity and selectivity measurements

Fischer–Tropsch synthesis was performed in a fixed-bed reactor (stainless steel, 10 mm inner diameter). The apparatus has been described in detail by Hilmen *et al.* [41]. The samples (1.0 g, 53–90  $\mu\text{m}$ ) were diluted with inert silicon carbide particles (4.0 g, 75–150  $\mu\text{m}$ ) in order to improve the temperature distribution along the catalytic zone. An aluminium jacket was placed outside the reactor to further reduce possible temperature gradients.

The samples were reduced *in situ* in hydrogen at ambient pressure while the temperature was increased at 1 K/min to 623 K. After 16 h of reduction, the catalysts were cooled to 443 K. The system was then pressurised at 20 bar and synthesis gas of molar ratio  $\text{H}_2/\text{CO} = 2.1$  (and 3%  $\text{N}_2$  as internal standard) was introduced to the reactor. To control the heat release and maintain the catalyst activity, the temperature was increased slowly to the reaction temperature 483 K. Space velocity was adjusted to give carbon monoxide conversion levels between 20 and 50 percent. Water vapour was intro-

duced by passing deionised water through an electrical vaporiser kept at 573 K and mixed with synthesis gas prior to the reactor inlet. The total pressure and the flow rate of synthesis gas were kept constant during external water addition. Thus, the partial pressures of the reactants were reduced as water was introduced in the feed stream.

Liquid products were removed in a cold trap, while heavy hydrocarbons were collected in a heated trap. The effluent gaseous product was analysed for hydrogen, nitrogen, carbon monoxide, carbon dioxide, water, and  $\text{C}_1$ – $\text{C}_9$  hydrocarbons using an HP5890 gas chromatograph equipped with a thermal conductivity detector (TCD) and a flame ionisation detector (FID).

The  $\text{C}_{5+}$  selectivity was calculated by subtracting the amount of  $\text{C}_1$ – $\text{C}_4$  hydrocarbons and carbon dioxide in the product gas mixture from the total mass balance. The activity is reported as the hydrocarbon formation rate ( $\text{g}_{\text{hydrocarbon}}/(\text{g}_{\text{catalyst}} \cdot \text{h})$ ).

## 3. Results and discussion

### 3.1. Support and catalyst characterisation

X-ray diffraction patterns of all supports confirm the presence of only  $\gamma\text{-Al}_2\text{O}_3$  [42]. Two examples (S-4 and S-5) are given in figure 1. These spectra are representative of all the other supports (S-1 to S-3). The patterns of the respective impregnated samples (C-4 and C-5) are presented in figure 2. In addition to the  $\gamma\text{-Al}_2\text{O}_3$  peaks, the catalysts exhibit reflections of  $\text{Co}_3\text{O}_4$  [42]. Apart from the peaks indicative of  $\gamma\text{-Al}_2\text{O}_3$  and  $\text{Co}_3\text{O}_4$ , the supported catalysts do not show any other peaks. Accordingly,  $\text{Co}_3\text{O}_4$  is the dominant crystalline cobalt species after calcination. No crystalline rhenium species are observed in the X-ray diffraction spectra. Cobalt metal

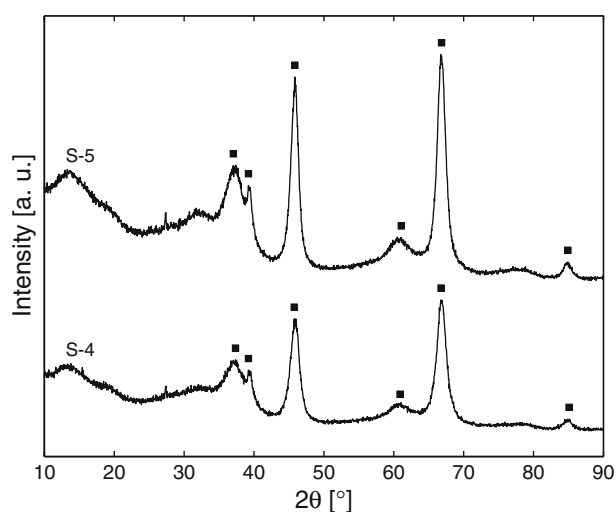


Figure 1. X-ray diffraction patterns of support S-4 and support S-5 (■ =  $\gamma\text{-Al}_2\text{O}_3$ ).

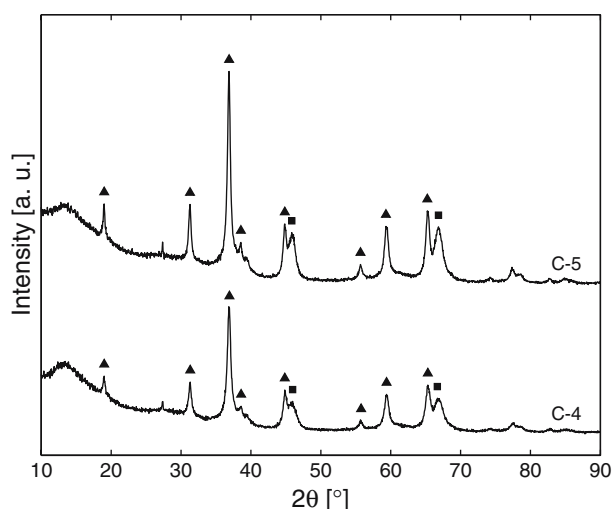


Figure 2. X-ray diffraction patterns of catalyst C-4 and catalyst C-5. Catalysts: 20 wt.% Co + 0.5 wt.% Re/ $\gamma$ -Al<sub>2</sub>O<sub>3</sub>. (■ =  $\gamma$ -Al<sub>2</sub>O<sub>3</sub>, ▲ = Co<sub>3</sub>O<sub>4</sub>).

particle sizes calculated from hydrogen chemisorption data and X-ray diffraction data are given in table 1.

Table 2 shows BET surface areas and pore size characteristics of the  $\gamma$ -Al<sub>2</sub>O<sub>3</sub> materials and the corresponding impregnated samples. The average pore diameters for the supports range from 7.4 to 20.8 nm, while the pore volumes are distributed in the interval 0.48–0.98 cm<sup>3</sup>/g. Introduction of cobalt to the supports decreases the surface area, the mean pore diameter, and the pore volume for all the supports as shown in table 2. In the remainder of this study, supports S-1 to S-4 will be referred to as “narrow-pore” supports, while S-5 will be denoted a “wide-pore” support. In the same way, catalysts C-1 to C-4 are “narrow-pore” catalysts while C-5 is a “wide-pore” catalyst.

To calculate the pore sizes, the BJH method was [39] applied. There exist a number of other techniques to

Table 1

Cobalt particle sizes of the calcined catalysts (20 wt.% Co + 0.5 wt.% Re/ $\gamma$ -Al<sub>2</sub>O<sub>3</sub>). The experimental error ( $\pm 2\sigma$ ) for the particle sizes calculated from X-ray diffraction data and chemisorption data is less than  $\pm 1$  nm and  $\pm 0.5$  nm, respectively

Catalyst	Co <sup>0</sup> particle size (nm)	
	X-ray diffraction <sup>a</sup>	Hydrogen chemisorption <sup>b</sup>
C-1	12	11
C-2	15	12
C-3	17	13
C-4	15	12
C-5	19	14

<sup>a</sup>  $d(\text{Co}^0) = 0.75 \cdot (d(\text{Co}_3\text{O}_4))$ ,  $d$  is the particle diameter.

<sup>b</sup>  $d(\text{Co}^0) = \frac{96}{D}$ ,  $D$  is the dispersion.

Table 2

Nitrogen sorption properties of  $\gamma$ -Al<sub>2</sub>O<sub>3</sub> supports (S) and the impregnated samples (C). Catalysts: 20 wt.% Co + 0.5 wt.% Re/ $\gamma$ -Al<sub>2</sub>O<sub>3</sub>. The experimental error ( $\pm 2\sigma$ ) is  $\pm 5$  m<sup>2</sup>/g for the surface areas,  $\pm 0.2$  nm for the mean pore diameters, and  $\pm 0.02$  cm<sup>3</sup>/g for the pore volumes

Sample	BET surface area (m <sup>2</sup> /g)	Mean pore diameter (nm)	Pore volume (cm <sup>3</sup> /g)
S-1	184	7.4	0.48
C-1	143	7.1	0.30
S-2	161	9.0	0.44
C-2	136	8.2	0.30
S-3	191	12.5	0.78
C-3	149	11.6	0.51
S-4	186	12.3	0.73
C-4	148	11.6	0.50
S-5	155	20.8	0.98
C-5	123	18.3	0.62

determine the pore size characteristics which are based on different assumptions and pore geometry. Thus, specific values will vary depending on the method, but the general findings are expected to be valid independent of any standard method employed.

### 3.2. Effect of water on the activity

The effect of water on the activity was studied by increasing the CO conversion, more precisely from 20–35 to approximately 50 percent. In addition, the influence of water was investigated by co-feeding different amounts of water,  $P_{\text{H}_2\text{O}}/P_{\text{H}_2} = 0.4$  and  $P_{\text{H}_2\text{O}}/P_{\text{H}_2} = 0.7$ , to the reactor inlet. On a molar basis, the two mentioned water levels correspond to 20 and 33 percent. In order to discover the extent of catalyst deactivation due to water exposure, the external water supply was stopped while the synthesis gas was kept flowing. Since the catalysts deactivate with time on stream irrespective whether water is introduced to the synthesis gas or not, experiments were also done without adding any water to the feed. Comparison of the “wet” and the “dry” experiments makes it possible to separate the contribution of the added water on the total deactivation. In total, the catalysts were kept on stream for a period of 140 h.

#### 3.2.1. Narrow-pore catalysts

Fischer–Tropsch synthesis reaction rates for catalyst C-4 are presented in figure 3. It is clear from figure 3 that continuous addition of small amounts of water decreased the activity for catalyst C-4. As the water concentration was increased from  $P_{\text{H}_2\text{O}}/P_{\text{H}_2} = 0.4$  to  $P_{\text{H}_2\text{O}}/P_{\text{H}_2} = 0.7$ , the negative effect of water on the activity was further strengthened. Although not presented graphically, the same scenario as described in figure 3 for catalyst C-4 was experienced for catalysts C-1 to C-3. Water decreased the reaction rate for all these catalysts.

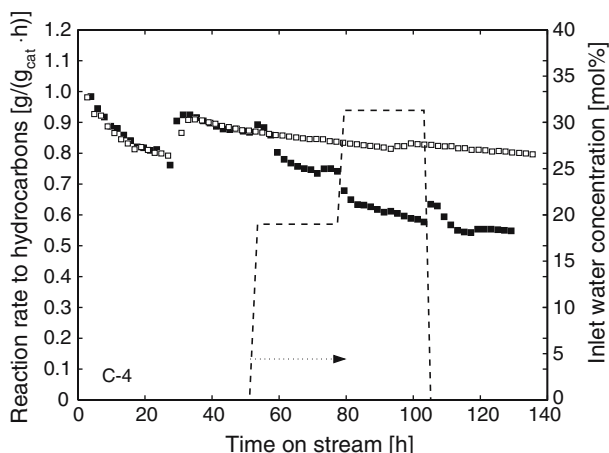


Figure 3. Reaction rate for formation of hydrocarbons vs. time on stream for catalyst C-4 (20 wt.% Co+0.5 wt.% Re/ $\gamma$ -Al<sub>2</sub>O<sub>3</sub>). (■ = water run, □ = dry run, - - = water concentration).

A negative impact on the Fischer–Tropsch activity for cobalt deposited on  $\gamma$ -Al<sub>2</sub>O<sub>3</sub> due to addition of water is consistent with previous findings [3–16]. It is known for similar catalysts that water may act as an oxidation agent, producing non-active cobalt. The extent of reoxidation depends on the partial pressure of water in the reactor. The reaction rate for catalyst C-4 was partially recovered immediately after removing water from the feed. This may be a result of an increase in the partial pressures of CO and H<sub>2</sub> on the reaction rate. The importance of the partial pressure values of CO and H<sub>2</sub> on the reaction rate is addressed in Section 3.2.3.

### 3.2.2. Wide-pore catalyst

The effect of water was also evaluated for catalyst C-5 at similar conditions as for catalysts C-1 to C-4. Fischer–Tropsch synthesis rates for catalyst C-5 are given in figure 4. In contrast to the narrow-pore  $\gamma$ -Al<sub>2</sub>O<sub>3</sub>

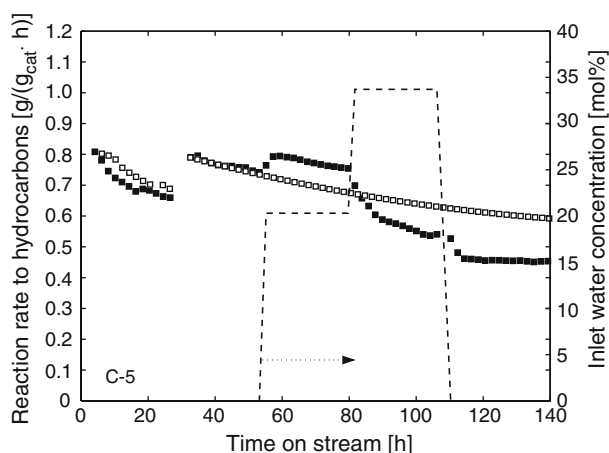


Figure 4. Reaction rate for formation of hydrocarbons vs. time on stream for catalyst C-5 (20 wt.% Co+0.5 wt.% Re/ $\gamma$ -Al<sub>2</sub>O<sub>3</sub>). (■ = water run, □ = dry run, - - = water concentration).

supported catalysts (C-1 to C-4), small amounts of externally provided water ( $P_{\text{H}_2\text{O}}/P_{\text{H}_2} = 0.4$ ) were in fact beneficial for the Fischer–Tropsch synthesis activity for the wide-pore catalyst. However, water had only a positive effect on the activity when it was present in relatively small quantities. Addition of larger amounts of water,  $P_{\text{H}_2\text{O}}/P_{\text{H}_2} = 0.7$ , decreased the reaction rate. Apparently, for the large-pore  $\gamma$ -Al<sub>2</sub>O<sub>3</sub> support, there exists an optimum value for the water concentration between  $P_{\text{H}_2\text{O}}/P_{\text{H}_2} = 0$  and  $P_{\text{H}_2\text{O}}/P_{\text{H}_2} = 0.7$ . When the water supply was terminated for catalyst C-5, the reaction rate decreased and then reached a pseudo steady-state value.

Although the supports were not  $\gamma$ -Al<sub>2</sub>O<sub>3</sub>, some other investigations have also shown increasing reaction rates with the addition of water. Krishnamoorthy *et al.* [26], for instance, reported that water increased the CO conversion rates for a Co/SiO<sub>2</sub> catalyst. They suggested that increased reaction rates were observed because water influenced the relative surface coverage of the active and inactive forms of carbon, present at low concentrations on the cobalt surfaces. Furthermore, Bertole *et al.* [27] investigated the effect of water vapour on Co and CoRe supported on TiO<sub>2</sub> and also on unsupported Co using carbon isotope transient at reaction steady-state. Increased CO reaction rates were found and according to Bertole *et al.* [27], water induced an acceleration of the CO dissociation rate. Dalai *et al.* [28] observed an increased CO conversion when water was added to a wide-pore SiO<sub>2</sub> supported cobalt catalyst. According to Dalai *et al.* [28], the effect of water depends on the pore size of the support, and also whether or not the cobalt clusters are small enough to fit inside the pores.

### 3.2.3. Impact of partial pressure of water for deactivation

Figures 3 and 4 clearly demonstrated that water and also the quantity in which it is present plays an important role for the Fischer–Tropsch synthesis activity. As mentioned before, Jacobs *et al.* [13,16] observed for various promoted and unpromoted  $\gamma$ -Al<sub>2</sub>O<sub>3</sub> supported cobalt catalysts that below 25 vol.%, no permanent deactivation of cobalt occurred. To validate the importance of the inlet water partial pressure, another experiment was designed for catalyst C-5. After approximately 26 h with water addition corresponding to  $P_{\text{H}_2\text{O}}/P_{\text{H}_2} = 0.4$  at the reactor inlet, the external water supply was removed. Figure 5 shows that after 140 h on stream, the reaction rate of the water exposed sample and the unexposed sample approached the same value. Thus, the water effect observed at low water amounts is most likely reversible, in accordance with Jacobs *et al.* [13,16].

Comparing reaction rates before and after external water addition gives a reliable estimate of the extent of deactivation. When the catalysts were exposed to inlet  $P_{\text{H}_2\text{O}}/P_{\text{H}_2} = 0.7$ , the reaction rates did not return to the



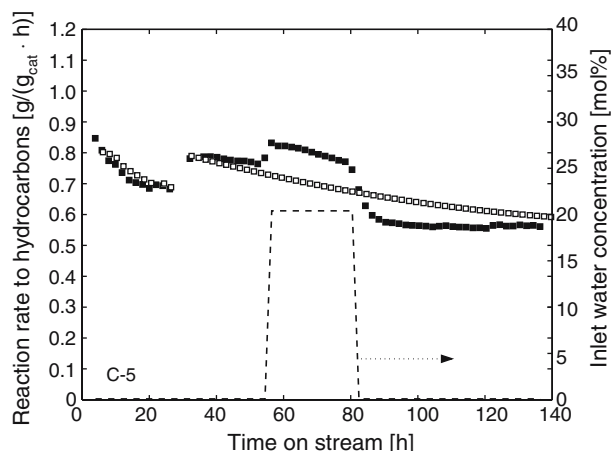


Figure 5. Reaction rate for formation of hydrocarbons vs. time on stream for catalyst C-5 (20 wt.% Co + 0.5 wt.% Re/ $\gamma$ - $\text{Al}_2\text{O}_3$ ). (■ = water run, □ = dry run, - - = water concentration).

same level as expected from the dry experiments as shown in figures 3 and 4. Accordingly, permanent deactivation of the catalysts seems to have occurred. This is in agreement with the results of Jacobs *et al.* [16] showing that irreversible deactivation occurs at sufficiently high concentrations of water (>25 vol.%). XANES scans of catalysts exposed to water indicated formation of species chemically resembling cobalt aluminate [13].

Since the total pressure was kept constant when water was co-fed along with synthesis gas, the partial pressures of hydrogen and carbon monoxide were reduced. Storsæter *et al.* [8] and Enger *et al.* [43] studied the effect of changes in the partial pressures of CO and  $\text{H}_2$  when water was added to the feed. Their results clearly showed that the reduced activity for catalysts C-1 to C-4 observed in this work can not be explained by reduced partial pressures of CO and  $\text{H}_2$ . For catalyst C-5, the activity actually increased despite the lower partial pressures during external water introduction ( $P_{\text{H}_2\text{O}}/P_{\text{H}_2} = 0.4$ ).

#### 3.2.4. Comparison of narrow-pore and wide-pore $\gamma$ - $\text{Al}_2\text{O}_3$ supported cobalt catalysts

The same effect of water as found for the wide-pore based catalyst has been observed for cobalt supported on wide-pore  $\text{SiO}_2$ ,  $\text{TiO}_2$ , and  $\alpha$ - $\text{Al}_2\text{O}_3$ . However, on  $\gamma$ - $\text{Al}_2\text{O}_3$ , an increased activity upon water addition has to our knowledge so far not been reported. Figure 3 shows that addition of small amounts of water to a narrow-pore catalyst reduced the reaction rates and figure 4 equally shows that for cobalt supported on wide-pore  $\gamma$ - $\text{Al}_2\text{O}_3$ , the presence of small amounts of water were beneficial for the reaction rates. Since these supports mainly differ in their pore characteristics and particle sizes, the structure of the support or the size/appearance of the cobalt crystallites seems to be important factors

for the role of water. Diffusion effects may contribute to the difference between narrow-pore supports and wide-pore supports. It has earlier been shown that the appearance of the cobalt particles depends on the support [44]. In the narrow-pore supports, cobalt seems to exist as clusters of small particles whereas for wide-pore supports such as  $\text{TiO}_2$ , cobalt exists as large particles when prepared by incipient wetness impregnation. Such a difference may explain the different behaviour with respect to water addition.

Dalai *et al.* [28] observed a similar phenomenon for narrow-pore and large-pore silicas with different cobalt loadings. While the catalyst activity of 12.4 wt.% cobalt on wide-pore  $\text{SiO}_2$  increased when water was introduced, addition of water to 20 wt.% Co on narrow- or wide-pore silica catalyst did not significantly alter the CO conversion. According to Dalai *et al.* [28], the water effects are influenced by the pore size of the silica support, and also whether or not the cobalt clusters are small enough to be located inside the pores. However, Krishnamoorthy *et al.* [26] indicated that the beneficial effect on CO conversion was not due to the removal of transport restrictions via the formation of intrapellet liquids at high water concentrations. Instead, Krishnamoorthy *et al.* [26] proposed that water possibly influences the relative concentration of the active and inactive forms of carbon present at low concentrations on Co surfaces.

#### 3.3. Effect of water on the selectivity

The product selectivity strongly depends on the level of conversion [7]. The selectivity of the different catalysts should therefore be compared at the same level of conversion rather than at constant space velocity.

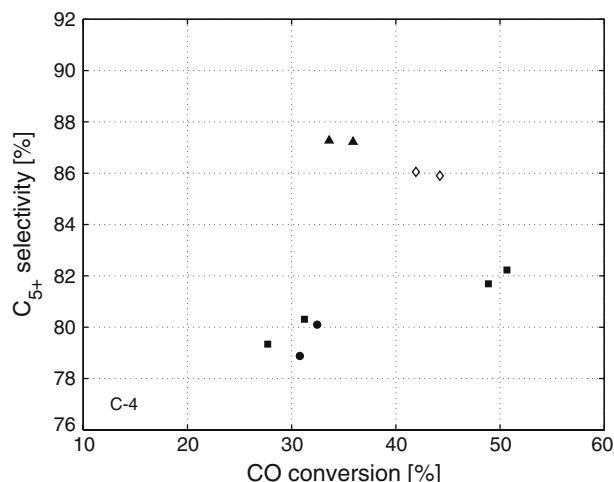


Figure 6.  $\text{C}_5^+$  selectivity vs. the CO conversion for catalyst C-4 (20 wt.% Co + 0.5 wt.% Re/ $\gamma$ - $\text{Al}_2\text{O}_3$ ) before, during, and after water addition (■ = before water addition, ◇ = 20% water, ▲ = 33% water, ● = after water addition).

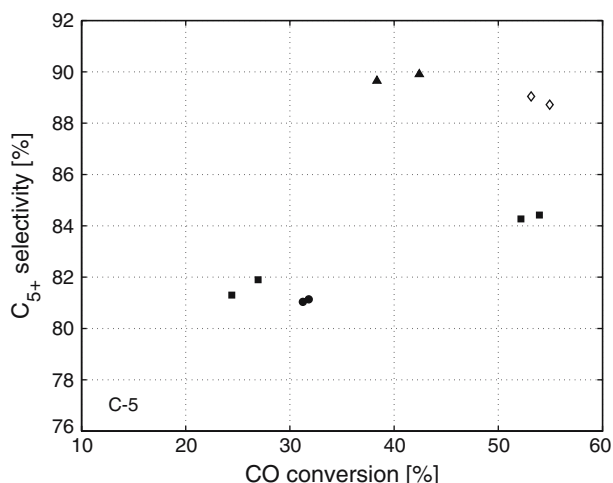


Figure 7. C<sub>5+</sub> selectivity vs. the CO conversion for catalyst C-5 (20 wt.% Co+0.5 wt.% Re/ $\gamma$ -Al<sub>2</sub>O<sub>3</sub> before, during, and after water addition (■ = before water addition, ◇ = 20% water, ▲ = 33% water, ● = after water addition).

The C<sub>5+</sub> selectivity as a function of the conversion of CO is shown in figure 6 for the narrow-pore supported catalyst (C-4) and in figure 7 for the wide-pore supported catalyst (C-5). The results include experiments at dry conditions, at two different water additions, and after removal of the water. The C<sub>5+</sub> selectivity increases as the CO conversion is increased or as water is cofed to the reactor. The effect of water on the selectivity is according to previous results [7–9,22–27,30–32]. Several different theories have been proposed for the effect of water on the selectivity. As already mentioned, Krishnamoorthy *et al.* [26] suggested that water influences the relative concentrations of active and inactive forms of carbon present at low concentrations on cobalt surfaces. Bertole *et al.* [27] proposed that a direct interaction between coadsorbed CO and water lowers the barrier to CO dissociation. The increased C<sub>5+</sub> selectivity is associated with an increase in the active carbon coverage caused by an increase in CO reactivity without a parallel increase in the overall activity of surface carbon. Recently, Bertole *et al.* [34] concluded from isotopic transient kinetic studies that the rate of propagation to termination during chain-growth is strongly correlated with the steady-state amount of active carbon for all carbon number products, and that the dominant form of active carbon is monomeric. They also concluded that most of the effects of changes in CO and water partial pressures on the chain-growth probability appear to arise via an indirect effect on the active carbon inventory.

#### 4. Conclusion

The effect of water on the activity and selectivity for a series of  $\gamma$ -Al<sub>2</sub>O<sub>3</sub> supported cobalt Fischer–Tropsch

catalysts was studied in an isothermal fixed-bed reactor at  $T=483$  K,  $P=20$  bar, and  $H_2/CO = 2.1$ . Addition of small amounts of water to a narrow-pore catalyst reduced reaction rates while for cobalt supported on  $\gamma$ -Al<sub>2</sub>O<sub>3</sub>, the presence of small amounts of water was beneficial for the reaction rates. For all the catalysts, water amounts equal to  $P_{H_2O}/P_{H_2} = 0.7$  at the reactor inlet suppressed the activity and resulted in permanent deactivation. Water increased the C<sub>5+</sub> selectivity and decreased the CH<sub>4</sub> selectivity for all catalysts. The pore characteristics most likely determine the effect of water on the activity.

#### Acknowledgments

The financial support from the Norwegian Research Council through the KOSK programme is greatly acknowledged. The authors also thank Statoil for financial support and for supplying alumina samples. Finally, Esther Ochoa Fernández is acknowledged for experimental assistance.

#### References

- [1] J.K. Minderhoud, M.F.M. Post, S.T. Sie and E.J.R. Sudholter, United States Patent 4,628,133 (1985).
- [2] J.K. Minderhoud, M.F.M. Post, S.T. Sie and E.J.R. Sudholter, European Patent Application 0,142,888 A2 (1985).
- [3] D. Schanke, A.M. Hilmen, E. Bergene, K. Kinnari, E. Rytter, E. Ådnanes and A. Holmen, Catal. Lett. 34 (1995) 269.
- [4] D. Schanke, A.M. Hilmen, E. Bergene, K. Kinnari, E. Rytter, E. Ådnanes and A. Holmen, Energy Fuels 10 (1996) 867.
- [5] A.M. Hilmen, D. Schanke and A. Holmen, Stud. Surf. Sci. Catal. 107 (1997) 237.
- [6] A.M. Hilmen, D. Schanke, K.F. Hanssen and A. Holmen, Appl. Catal. A. 186 (1999) 169.
- [7] A.-M. Hilmen, O.A. Lindvåg, E. Bergene, D. Schanke, S. Eri and A. Holmen, Stud Surf Sci Catal. 136 (2001) 295.
- [8] S. Storsæter, Ø. Borg, E.A. Blekkan and A. Holmen, J. Catal. 231 (2005) 405.
- [9] S. Storsæter, Ø. Borg, E.A. Blekkan, B. Tøtdal and A. Holmen, Catal. Today 100 (2005) 343.
- [10] M. Rothaemel, K.F. Hanssen, E.A. Blekkan, D. Schanke and A. Holmen, Catal. Today 38 (1997) 79.
- [11] G. Jacobs, P.M. Patterson, Y. Zhang, T. Das, J. Li and B.H. Davis, Appl. Catal. A. 233 (2002) 215.
- [12] T.K. Das, G. Jacobs, P.M. Patterson, W.A. Conner, J. Li and B.H. Davis, Fuel 82 (2003) 805.
- [13] G. Jacobs, P.M. Patterson, T.K. Das, M. Luo and B.H. Davis, Appl. Catal. A 270 (2004) 65.
- [14] P.J. van Berge, J. van de Loosdrecht, S. Barradas and A.M. van der Kraan, Catal. Today 58 (2000) 321.
- [15] J. Li, X. Zhan, Y. Zhang, G. Jacobs, T. Das and B.H. Davis, Appl. Catal. A 228 (2002) 203.
- [16] G. Jacobs, T.K. Das, P.M. Patterson, J. Li, L. Sanchez and B.H. Davis, Appl. Catal. A 247 (2003) 335.
- [17] G.W. Huber, C.G. Guymon, T.L. Conrad, B.C. Stephenson and C.H. Bartholomew, Stud. Surf. Sci. Catal. 139 (2001) 423.
- [18] J.-G. Chen, X.-Z. Wang, H.-W. Xiang and Y.-H. Sun, Stud. Surf. Sci. Catal. 136 (2001) 525.
- [19] J. Li, G. Jacobs, T. Das and B.H. Davis, Appl. Catal. A 233 (2002) 255.

- [20] G. Kiss, C.E. Klierer, G.J. DeMartin, C.C. Culross and J.E. Baumgartner, *J. Catal.* 217 (2003) 127.
- [21] T.K. Das, W.A. Conner, J. Li, G. Jacobs, M.E. Dry and B.H. Davis, *Energy Fuels* 19 (2005) 1430.
- [22] C.J. Kim, European Patent Specification 0,339,923 B1 (1989).
- [23] C.J. Kim, European Patent Application 0,335,218 A1 (1990).
- [24] Kim C.J., United States Patent 5,227,407 (1993).
- [25] H. Schulz, E. van Steen and M. Claeys, *Stud. Surf. Sci. Catal.* 81 (1994) 455.
- [26] S. Krishnamoorthy, M. Tu, M.P. Ojeda, D. Pinna and E. Iglesia, *J. Catal.* 211 (2002) 422.
- [27] C.J. Bertole, C.A. Mims and G. Kiss, *J. Catal.* 210 (2002) 84.
- [28] A.K. Dalai, T.K. Das, K.V. Chaudhari, G. Jacobs and B.H. Davis, *Appl. Catal. A* 289 (2005) 135.
- [29] J. Li, G. Jacobs, T. Das, Y. Zhang and B. Davis, *Appl. Catal. A* 236 (2002) 67.
- [30] S. Eri, K.J. Kinnari, D. Schanke and A.-M. Hilmen, International Publication Number WO 02/47816 A1 (2002).
- [31] E. Iglesia, *Appl. Catal. A* 161 (1997) 59.
- [32] H. Schulz, M. Claeys and S. Harms, *Stud. Surf. Sci. Catal.* 107 (1997) 193.
- [33] C. Aaserud, A.-M. Hilmen, E. Bergene, S. Eri, D. Schanke and A. Holmen, *Catal. Lett.* 94 (2004) 171.
- [34] C.J. Bertole, G. Kiss and C.A. Mims, *J. Catal.* 223 (2004) 309.
- [35] H.P. Klug and L.E. Alexander, *X-ray Diffraction Procedures* (Wiley, New York, 1976).
- [36] D. Schanke, S. Vada, E.A. Blekkan, A.M. Hilmen, A. Hoff and A. Holmen, *J. Catal.* 156 (1995) 85.
- [37] E. Rytter, D. Schanke, S. Eri, H. Wigum, T.H. Skagseth and N. Sincadu, *ACS Petrol. Chem. Div. Prepr.* 47 (2002).
- [38] S. Brunauer, P.H. Emmett and E. Teller, *J. Am. Chem. Soc.* 60 (1938) 309.
- [39] E.P. Barrett, L.G. Joyner and P.P. Halenda, *J. Am. Chem. Soc.* 73 (1951) 373.
- [40] R.C. Reuel and C.H. Bartholomew, *J. Catal.* 85 (1984) 63.
- [41] A.-M. Hilmen, E. Bergene, O.A. Lindvåg, D. Schanke, S. Eri and A. Holmen, *Catal. Today* 105 (2005) 357.
- [42] *DIFFRAC<sup>plus</sup> EVA Release 2001 Version 7.0 rev.0*, Bruker AXS, 2001.
- [43] B.C. Enger, V. Frøseth, Ø. Borg, E. Rytter and A. Holmen, submitted.
- [44] S. Storsæter, B. Tøtdal, J.C. Walmsley, B.S. Tanem and A. Holmen, *J. Catal.* 236 (2005) 139.